Some Examples of Incomplete Diagnostic Analyses of Industrial Machinery

Nicolò Bachschmid(✉)

Department of Mechanics, Politecnico di Milano,
via LaMasa 1, 20158 Milano, Italy
nicolo.bachschmid@polimi.it

Abstract. Diagnostic tasks on industrial machinery can sometimes be dealt basing only on previous experience with successful model based identification techniques. This may be required when necessary time and resources for complete diagnostic analysis are not available. Some examples of machines affected by malfunctions that have been more or less successfully analyzed, often without resorting to machine specific models, are presented. Journal ovalisation in a HP-IP steam turbine was identified in the first example, the vibration changes in a LP steam turbine could be attributed to coupling misalignment and to a loose last stage blade of the shaft in the second example. Rubs and thermal bow combined to axial shaft expansion restriction could explain the severe vibrational behavior of a steam turbine that prevented its operation in a third example. The abnormal noise of a vertical shaft generator of a hydroelectric power plant was attributed to a structural resonance excited by electromagnetic forces in a third example, where the diagnostic process was completed by validating the complex excitation mechanisms with simulations.

Keywords: Vibrations · Diagnostics · Malfunction identification
Industrial machinery

1 Introduction

In industrial environment it may occur that unexpected vibrational behavior or excessive noise starts to affect rotating machineries after a major overhaul or refurbishment. Automatic diagnostic tools such as model based identification software, although available at reasonable costs, are often not installed originally in the plant surveillance system. Adaptation to the specific plant and installation of such diagnostic software requires time (some months) for software implementation and hardware installation. Time loss and costs for a single application are often believed by the plant management to be not affordable.

Plant management and/or machine manufacturers then often ask universities or consultants for help in analyzing the problem and propose solutions. More accurate and extended measurements and suitable acquisition systems are then generally required, in order to define at the best the vibrational behavior of the machine. To complete and validate the analysis a model of the machine and of the malfunction should be built to reproduce with the model the experimental behavior. This additional step for

K. L. Cavalca and H. I. Weber (Eds.): IFToMM 2018, MMS 61, pp. 191–206, 2019.
https://doi.org/10.1007/978-3-319-99268-6_14

completing the diagnosis requires of course additional costs. All these reasons make sometimes the complete diagnostic procedure not feasible.

Expert analysts are therefore called to give suggestions based on own knowledge acquired by means of previous theoretical analyses and experimental results. In this paper some examples of machines affected by malfunctions that have been more or less successfully analyzed without resorting to machine specific models, due to lack of time and resources, are presented. A case where instead additional tests have been performed and suitable machine specific models have been used for validating the complete diagnostic procedure, that otherwise would have been unsuccessful, is finally presented.

2 Four Case Histories

Three examples of machines affected by malfunctions that have been analyzed without resorting to diagnostic tools and machine specific models, are presented.

The first example is related to the shaft of the HP-IP section of a two casing steam turbine used in a cogeneration plant where variable operating conditions with many stops and restarts were required. A crack was initially suspected due to a consistent 2X component in the bearing vibrations and provisions were established for controlling its possible propagation. A complete model based diagnosis could have identified position and depth of the crack as for instance described in [1]. A deeper analysis revealed instead that the 2X component was mainly due to a journal out of roundness.

In the LP section of the same turbo-group the abnormal 1X vibration behavior consisting in rather high amplitudes in the whole speed range, as well as consistent amplitude variations in a small speed range close to the rated speed, was attributed to misalignment, and realignment of the complete group was decided. But during a standard visual inspection of the last stage blades a loose blade was discovered that generated the abnormal behavior. A complete diagnosis would have determined quantitatively the effects of unbalance and misalignment change for validating the results, as it is described for instance in [2].

The third example is a 100 MW turbo-group that could not be operated due to excessive vibration amplitudes, after an overhaul. Plant management asked for crack analysis. Rubbing and thermal bow were instead suspected; the bow was confirmed by measurements during slow rolling. But the sharp increase of vibrations indicated an additional cause, that was finally identified as shaft axial thermal elongation restriction.

The last example is the vertical shaft hydrogenerator, affected by abnormal high noise emission after the substitution of stator and rotor with some small modification with respect to the original machine. Measurements showed that the noise was generated by rather high vibrations of the structure at 700 Hz. The cause of excitation was identified, the response of the structure was amplified by a resonant condition that could be confirmed by additional tests. Amplitudes of excitation were simulated with suitable models and dedicated software, as well as the dynamic response of the structure and the noise emission. This way the complete diagnostic procedure has been validated by simulations reproducing electromagnetic behavior, mechanical behavior and acoustical behavior.

2.1 Behavior of a HP-IP Steam Turbine Rotor

The rotor of the HP-IP section of the two casing steam turbine of a cogeneration plant is supported by 2 tilting pad bearings, each one as usual equipped with two proximity probes according to +45° and −45° directions with respect to the vertical.

Figure 1 shows the Bode diagrams in which 1X and 2X amplitudes of the four sensors and related phases as function of the rotating speed during the run up, in the actual condition.

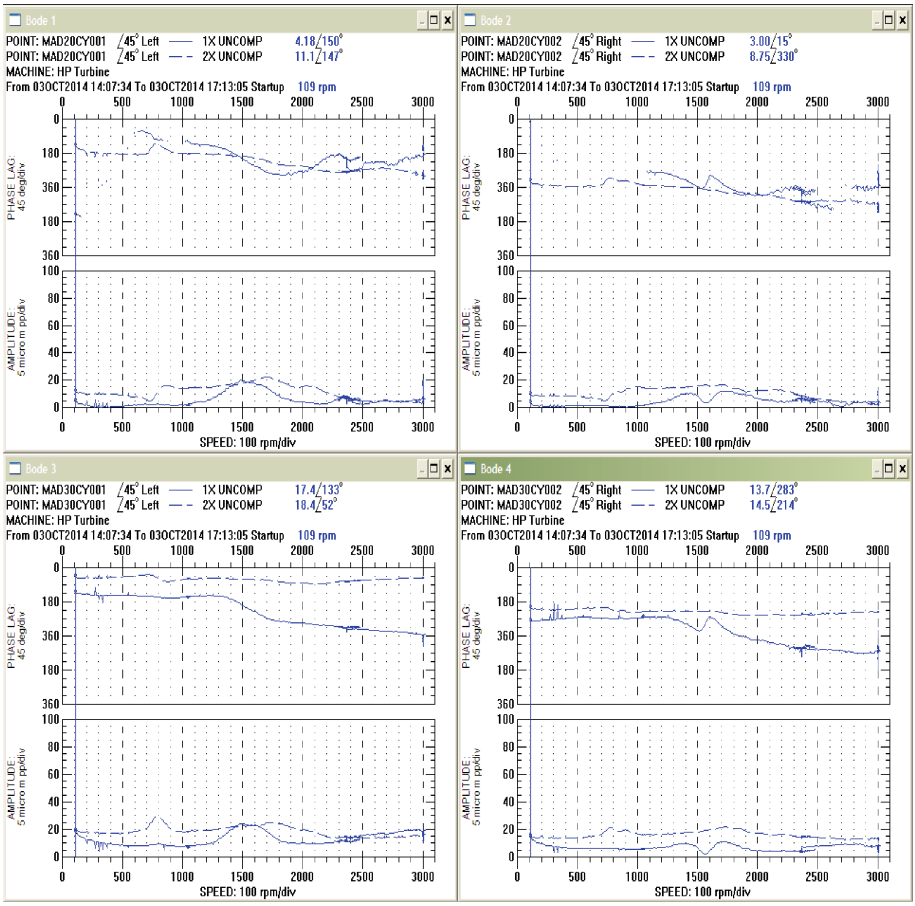

Fig. 1. 1X and 2X amplitudes and phases during a startup *after realignment* of HP-IP turbine

The supports and shafts of the complete group had been realigned during a maintenance stop, because a foundation settlement had been discovered.

Figure 2 shows the same diagrams that were recorded during a startup before the maintenance stop. Small differences in behavior are obviously due to little different thermal conditions of the rotor during the startup transients.

Impressive are the differences in the 1X behavior, the huge reduction of the vibration amplitudes, especially in the second bearing which, being close to the coupling flanges of the LP section of the machine, is mostly sensitive to the bearing/support alignment of the complete machine.

In reality it will be shown that the malfunction affecting the LP turbine described in the next section has also a significant effect on the vibrations of the HP-IP turbine shaft in the high speed range, which disappears when the malfunction is removed.

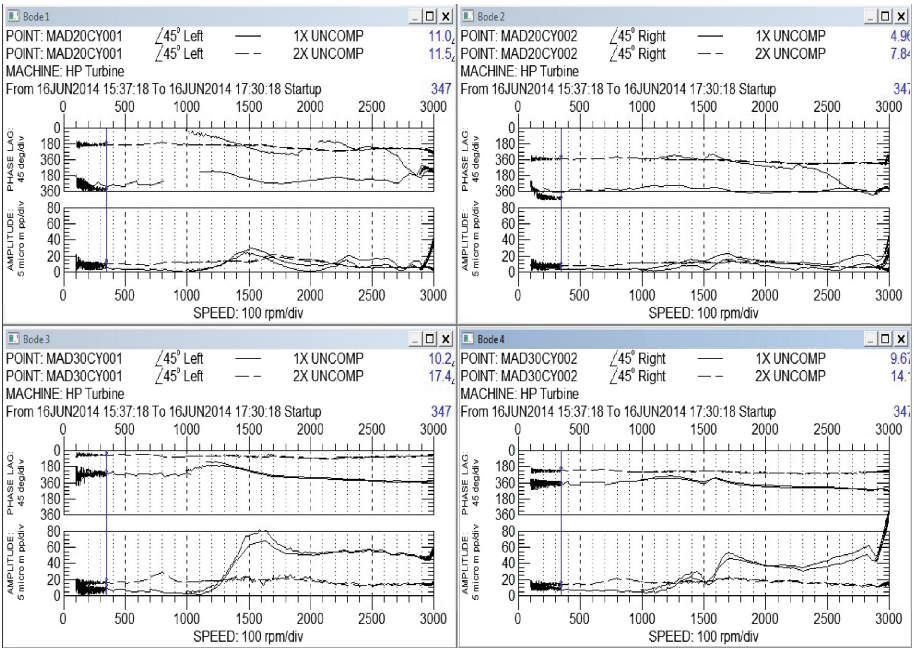

Fig. 2. 1X and 2X amplitudes and phases during a startup *before realignment* of HP-IP turbine

Interesting is the analysis of the 2X component which seems to be rather insensitive to alignment conditions, having similar trends before and after realignment. On the second bearing the 2X amplitude is something less than 20 μm in the all speed range except when crossing the secondary resonance at 750 rpm, half the critical speed, where some dynamic magnification is recognizable. The phase of this component is rather constant in the complete speed range.

2X components can be due to different causes, disregarding in this case flexible coupling misalignment, being the shafts coupled with rigid flanges:

(i) Journal ovalization (out of roundness)
(ii) Oil film non-linearity
(iii) axially unsymmetrical shaft stiffness (as caused by cracks f.i.).

Each cause generates specific features that allow to distinguish among the different malfunctions.

(i) Ovalization generates at low rotational speeds, when dynamic effects can be disregarded, 2X components with a relative phase of 180° (corresponding to a shaft rotation of 90°) in the 2 sensors that have an offset of 90° as described for instance in [3]. Dynamic effects are hardly recognizable, which means that amplitude and phase are changing very little with speed. This is exactly the situation in the above diagrams: phase is rather constant and phase shift between the two sensors is close to 180°.
(ii) Oil film non-linearity appears and generates 2X components when 1X components in the bearing are huge due to high unbalance or little damped critical speeds, or when bearing loads are high due to heavy misalignment, as described again in [3]. The 2X component then follows the trend of the 1X component. This cause can be excluded because, while 1X component amplitude is changing a lot with speed and between the two startups, the 2X component is always rather constant.
(iii) Axially unsymmetrical shaft stiffness generates at low speed 2X components with a phase shift of only 90° (corresponding to a shaft rotation of 45°). These components are further very sensitive to dynamic effects such as amplitude magnification and huge phase variations at secondary critical speeds, as described in [1]. In above diagrams we have rather small amplitude magnifications and phase variations in correspondence of the secondary critical speed, that could exclude the presence of a significant crack.

The feared possibility of a transverse crack in the rotor could be discarded attributing the 2X behavior to the out of roundness of the journals. Nevertheless continuous monitoring of the 2X component was recommended for detecting possible changes that could indicate the propagation of a crack.

2.2 Behavior of a LP Steam Turbine Rotor

The double flow LP steam turbine rotor, shown in Fig. 3, was supported on two lemon shaped bearings, each one equipped with two proximity probes. The measurements showed a behavior with rather high vibration amplitudes, especially on the bearing which was close to the connecting flange with the HP-IP rotor, which also was affected by high vibrations in the higher speed range. This behavior was attributed to an angular and radial misalignment of the two shafts due to coupling flange tightening after a foundation settlement that had been discovered and measured only recently.

Fig. 3. Double flow low pressure steam turbine rotor after finishing at factory

The Bode diagrams of the four sensors shown in Fig. 4 were recorded during a startup before the maintenance stop required to realign the machines.

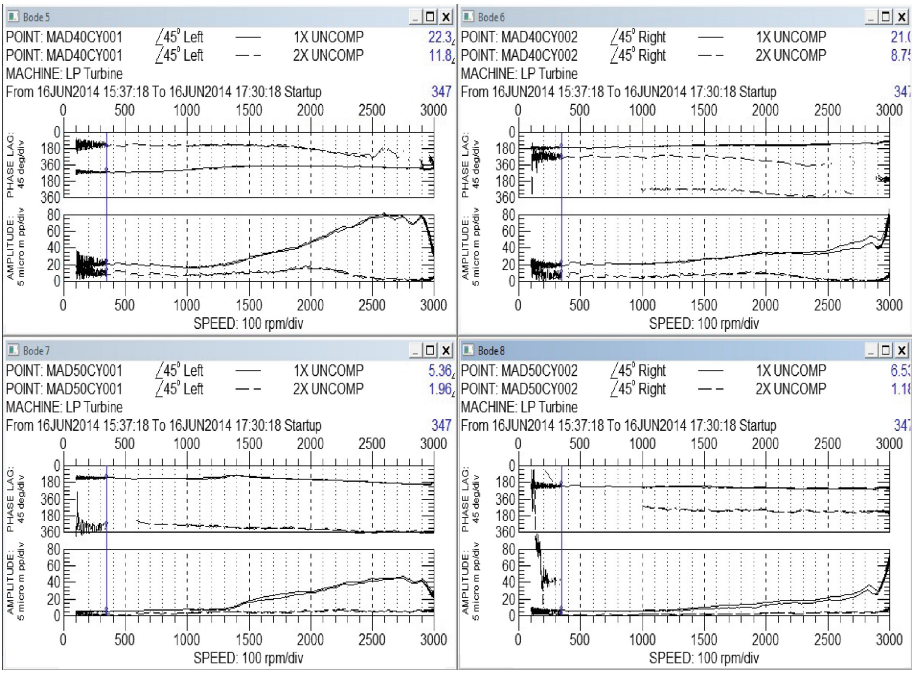

Fig. 4. 1X and 2X amplitudes and phases during a startup before realignment in LP turbine

Looking closely to the diagrams of the first bearing, it can be noted that at increasing rotational speed the 1X amplitudes increase up to the speed 2600 rpm, with no change in the phase, that indicates poor dynamic behavior with no evident critical

speed crossing. This trend is consistent with a misalignment, that can be conveniently modelled as an external rotating bending moment with constant amplitude [2]. This generates also the constant 1X amplitude of 20 μm at very low speed. Above 2600 rpm the vibration amplitude increase is opposed by some dynamic effect which prevails in the last 100 rpm before reaching the rated speed of 3000 rpm. A similar effect but in opposite direction is recognizable on the second sensor of the first bearing. The other bearing shows the same behavior although with smaller amplitudes. This huge dynamic effect might be attributed to some unbalance which opposes its centrifugal force (proportional to the square of the rotational speed) to the misalignment effect in an effective way only in the higher speed range close to the rated speed of the machine. Also the HP-IP rotor bearing on the load side is involved in this strange behavior by means of the coupling.

During the standard inspection of the last stage blade row through a window in the casing, it was discovered with surprise that the closing blade of the last row had moved along its seat from its original position for roughly 30 mm in axial direction.

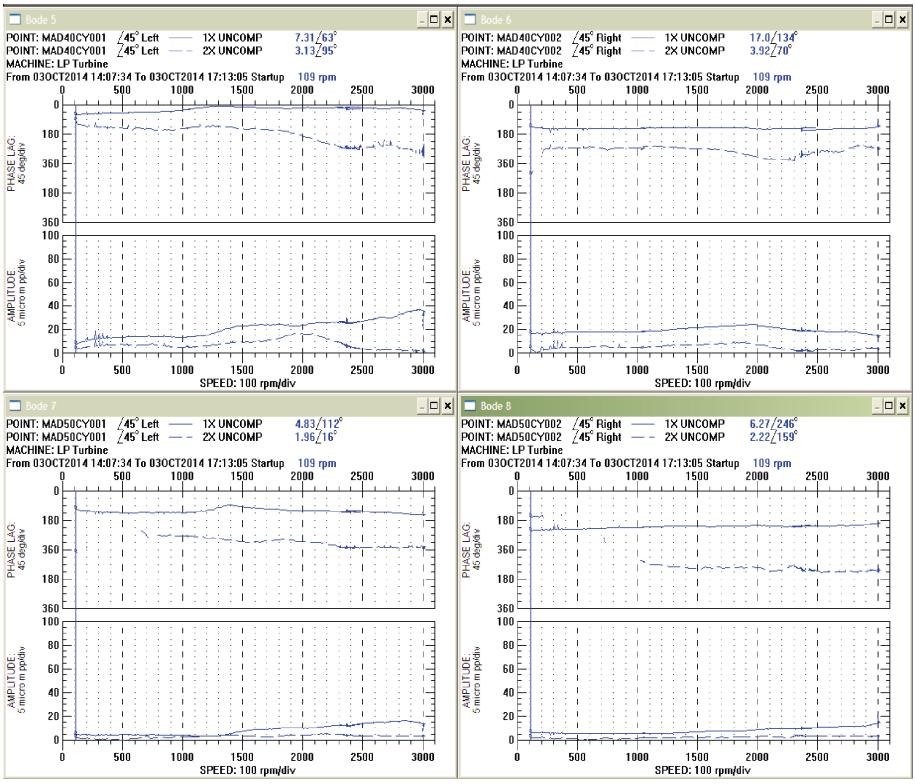

Fig. 5. 1X and 2X amplitudes and phases during a startup after realignment in LP turbine

This displacement generates a change in the balance situation of the rotor which is equivalent to a rotating bending moment with amplitude proportional to the square of the speed. The bending moment at rated speed evaluated with these data resulted to be roughly 10^5 Nm, a value which is consistent with the generated vibrations.

The phase shift between the two bearings of the 1X component is close to 180° which supports the assumption of the huge local bending moment acting on the shaft.

Figure 5 shows the diagrams of the same bearings which were obtained during the startup after having aligned accurately the shafts and having fixed the blade in its proper position.

It can be seen that a huge reduction in vibration amplitude has been obtained by proper alignment and by fixing the blade in its original position.

The strange dynamic behavior at rotational speeds close to the rated speed disappeared completely. The reduction of the 1X component at low speed was rather small, which could indicate the presence of a small permanent bow or that the alignment could be still improved.

The models of the rotor system, of the unbalance and of the misalignment would have allowed to simulate and validate both malfunctions, as it has been done in [2], but the management of the plant did not want to dedicate additional resources to the validation and deemed the obtained results satisfactory.

2.3 Behavior of the 100 MW Steam Turbine Rotor

The 100 MW power generation group shown in Fig. 6 while increasing output power after a smooth start up transient, suddenly reached trip level in the turbine bearing.

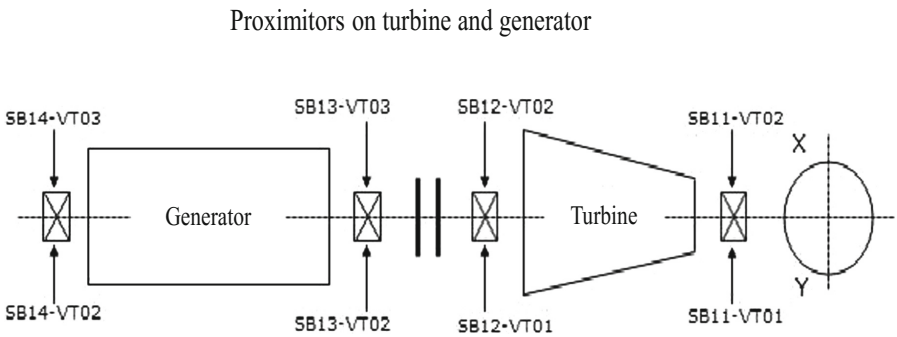

Fig. 6. Sketch of the 100 MW power generation group.

Figure 7 shows the time history of all vibrations of turbine and generator during this event. Vibration of free end of steam turbine starts to increase and reaches trip level after around 30 min. During the run down at critical speed still higher amplitudes are reached in almost all sensors and at low speed vibrations that are higher than at rated

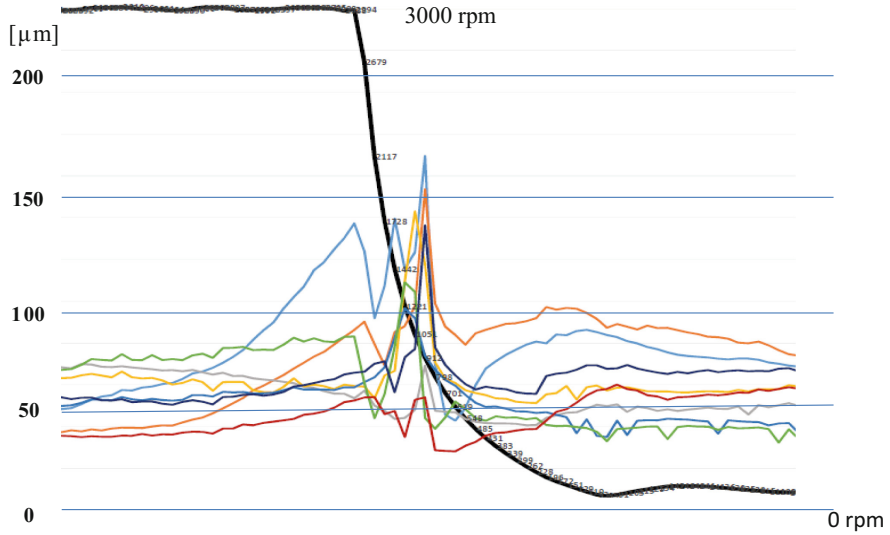

Fig. 7. Vibration time histories (during 60 min) before and after trip: orange and blue curves are related to the free end turbine bearing, dark red and dark grey are related to the other turbine bearing, **black** line indicates the rotational speed.

speed are measured in all sensors of the turbine. The behavior during and after the run down is consistent with a thermal bow, which was confirmed by the plant management: before starting again the turbine, the rotor needed to be slowly rolled for 20 h, in order to reduce and equalize the thermal stresses. Regarding the cause of the thermal bow it can be assumed that it has been most likely generated by severe rubs in some sealing. The rising of amplitude in 30 min is consistent with that hypothesis, as can be deduced from analysis described in [4].

At the following startup (2 days later) the behavior was similar but with a much sharper increase of vibrations (trip level was reached in 5 min), higher vibration amplitudes (with a peak at 240 μm) in passing the critical speed and higher residual vibrations at low speed, as shown in Fig. 8.

What has changed in the machine? Was it a much more severe rub, that generated a much greater bow? Or was there an additional cause that changed the vibrational behavior so much? Difficult to decide, since additional information like Bode diagrams with amplitude and phase of 1X and 2X components or journal orbits in the bearings were not available. The only available additional data were some spectra at rated speed, which showed the presence also of a consistent 2X component that could have been generated by a crack in the rotor.

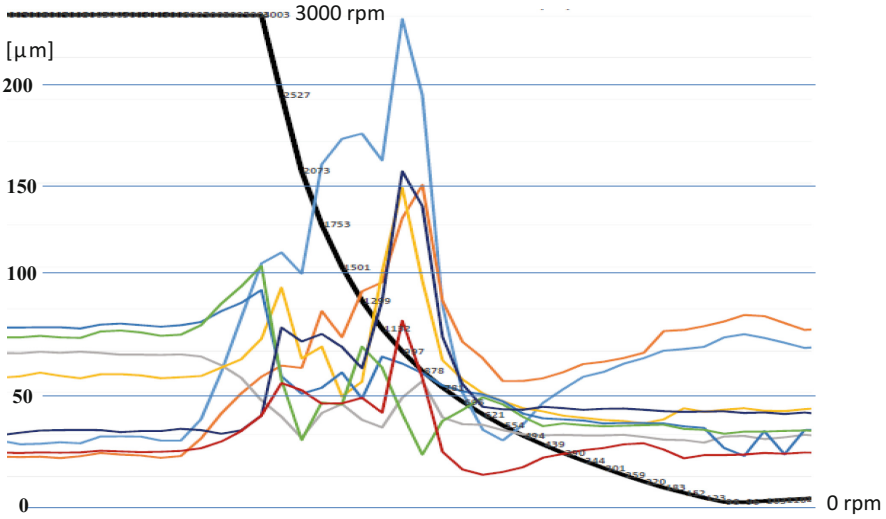

Fig. 8. Vibration time histories (during 42 min) before and after trip: orange and blue curves are related to the free end turbine bearing, dark red and dark grey are related to the other turbine bearing, **black** line indicates the rotational speed.

A deeper analysis was proposed to the management of the plant that rejected the proposal, preferring to get a deeper insight of the malfunction with additional trial runs and inspections. A complete diagnostic analysis of the malfunction would have been useful for not wasting time and money with trial and error procedures.

It was finally discovered that the axial elongation of the shaft due to heating, at the increasing of output power, had been restricted by error after the overhaul. This caused the bending and rubbing of the shaft. After having removed the axial restriction the machine could be operated smoothly at full power.

2.4 Behavior of a Vertical Shaft Hydrogenerator

The generator of the 55 MW vertical shaft hydrogenerator shown in Fig. 9 had been partially rebuild introducing some smaller changes in the design of the machine.

Characteristics of the machine: rotational speed is n_r = 136,66 rpm, number of slots in the stationary pack n_s = 330 (that was 360 in the previous design), number of pole pairs n_p = 22.

At the startup of the group, huge noise was measured close to the casing of the machine and also in the control room. The noise was produced in all different operating conditions with only small changes in amplitude: at load and no-load, with excitation and without excitation.

The problem of noise emission in this kind of electrical machines is well known since a long time, as can be seen in literature by reading e.g. [5]

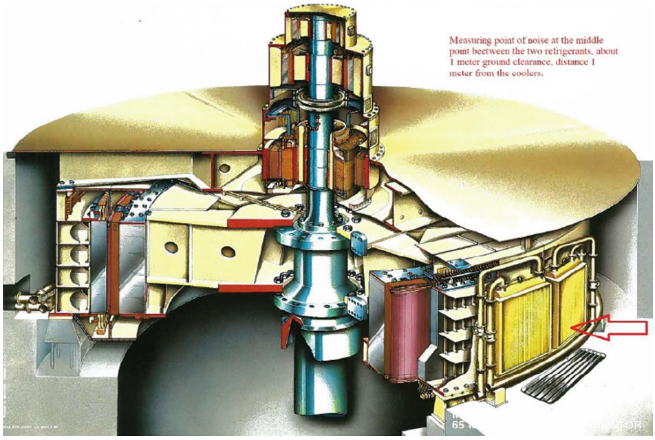

Fig. 9. Sketch of the generator: arrow indicates the noise measurement point.

Figure 10 shows the noise measurement results, at rated speed in 3 different operating conditions: without excitation, with excitation and no output power, with excitation and a power output of 31 MW.

At the frequency of 800 Hz the noise reaches 105 dB when the machine is excited, both with and without load, and something less, 102 dB, when the machine is without excitation. The reason why, even without excitation, the measured noise was so high could not be clarified. At the frequency of 700 Hz direct noise measurements were not taken; but we have measurements at 650 Hz, which show that the differences among the 3 different conditions are higher: the maximum is reached by the condition of load.

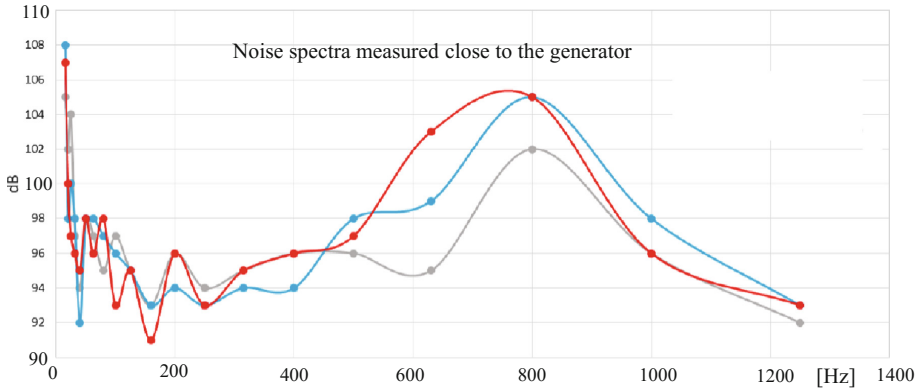

Fig. 10. Frequency analysis of noise in 3 different conditions: grey without excitation, blue with excitation but no load, red with excitation and 31 MW load.

Noise spectra in the control room were similar but obviously levels were lower, but still very unpleasant: 85–86 dB at 800 Hz when excited and 76 dB without excitation.

Independently of the cause of the severe noise emission, is was mandatory to provide means to reduce the noise at least in the control room.

Very interesting are the vibration measurements on the casing of the generator shown in Fig. 11 in case of no excitation (left) and with excitation (right). Due to the excitation the vibration velocity at 700 Hz jumps from 0.01 mm/s to 1.2 mm/s and at 800 Hz from a similar value to 0.6 mm/s.

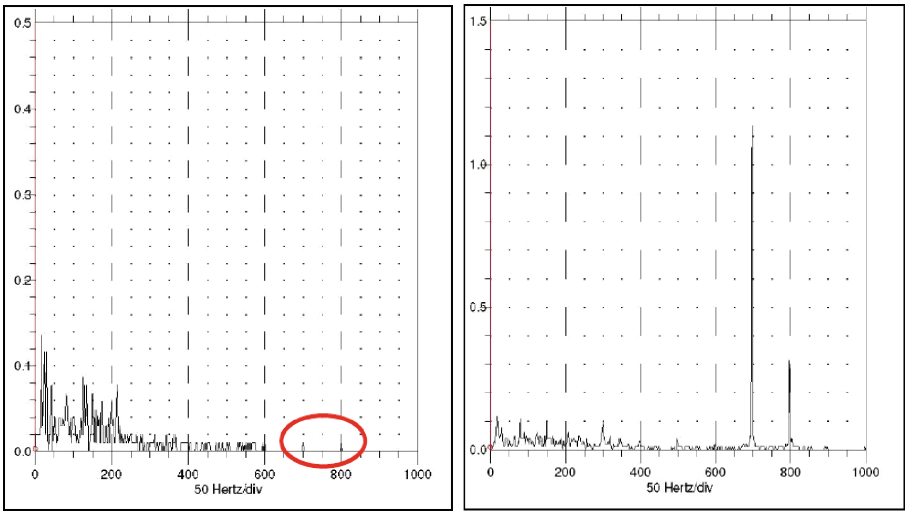

Fig. 11. Vibration spectra of generator casing: left without excitation, right with excitation

When power is generated the vibrations increase. Measurements were taken also on the core pack structure, where the vibrations reached a maximum of 2.6 mm/s in radial direction and 1.2 mm/s in axial direction at 700 Hz.

The high noise associated with these vibration velocities values indicate that the vibration mode shape of the structure has probably a high radiation efficiency.

Unfortunately it was not possible to have further information about the distribution of the vibrations over the casing surface, therefore the vibration mode at 700 Hz could not be experimentally identified.

Now let's analyze the source of excitation: in the stator we have n_s slots, the electromagnetic forces generated by the current in the coils of the rotor are rotating with the rotor speed corresponding to the frequency f_r: the excitation frequency f_e is therefore:

$$f_e = n_s f_r \tag{1}$$

being $f_r = n_r/60 = 2.275$ Hz, the stator is excited by frequency $f_e = 330 \times 2.275 = 750$ Hz. Taking account that the exciting rotating magnetic field with n_p pairs of poles is periodical with a period which is 1/22 of one revolution, the resulting force has a frequency $f_g = f_r\, n_p = 2.275 \times 22 = 50$ Hz. The force acting on the stator is therefore modulated by this frequency. As a result we have two resulting exciting frequencies:

$$f_e^I = 750 + 50 = 800 \text{ Hz} \qquad f_e^{II} = 750 - 50 = 700 \text{ Hz} \tag{2}$$

The excitation forces at the above frequencies are not the only responsible for the huge vibration amplitudes generated, since there was supposedly a consistent magnification factor at least at the frequency of 700 Hz, due to a mechanical resonance of the stator.

The excitation mechanism is similar to the blade row excitation in steam turbines, with the difference that here the excitation is rotating and the vibration is a travelling wave on the stator, whilst in a rotating blade row the excitation is the stationary pressure field that generates a backward travelling wave in the blade row.

Resonance in periodical structures occurs when excitation frequency equals the natural frequency, but only when also the harmonic order of the exciting force spatial distribution is equal to the number of nodal diameters of the natural vibration mode, as described f.i. in [6].

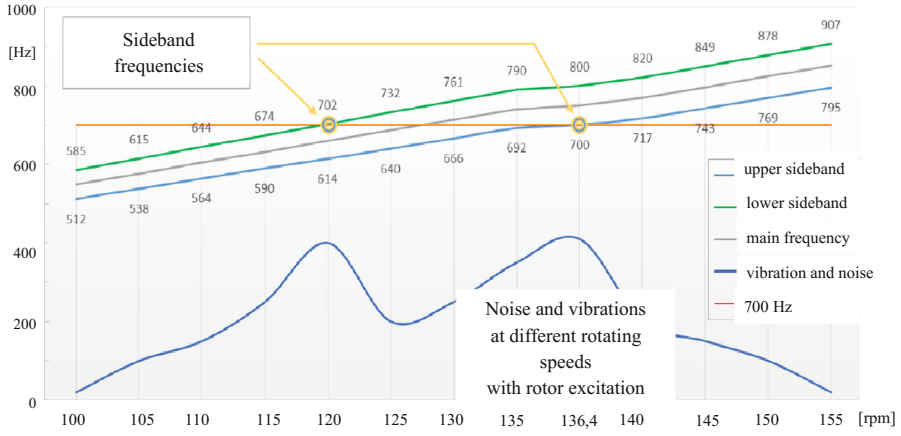

Fig. 12. Noise and vibrations at changing rotational speeds, with external rotor excitation.

The stator resonance could be proved experimentally by changing the rotational speed whilst the rotor coil current was fed by means of an external current generator. This resonance was not excited in the original design of the machine that had 360 slots instead of 330 slots. This generated a shift of around 10% in the exciting frequencies.

Figure 12 shows the results of noise measurements at different rotational speeds. Two peaks are obtained at the rotational speeds of 120 rpm and of 136.4 rpm, the last one is the rated operating speed of the generator. Maximum noise (and vibrations) are obtained when one or the other of the above exciting frequencies was equal to 700 Hz: this suggests that at that frequency a resonant condition is likely to occur.

In fact at the rotational speed of 120 rpm (2 Hz) the exciting frequency is:

$$f'_e = n_s f'_r = 330 \times 2 = 660 \text{ Hz}$$

and the rotating magnetic field has a frequency of:

$$f'_g = f'_r n_p = 2 \times 22 = 44 \text{ Hz}$$

which generates 2 exciting frequencies:

$$f_e^I = 660 + 44 = 704 \text{ Hz} \qquad f_e^{II} = 660 - 44 = 616 \text{ Hz} \tag{3}$$

At the rotational speed of 120 rpm we have again a resonance at 704 Hz similar to that one at the rated speed of the machine.

A finite element model of the stator has been set up exploiting the cyclic symmetry conditions: a sector corresponding to 1/10 of the complete axially symmetrical body has been considered. The boundary conditions were difficult to estimate, as a first approach fixed boundary conditions in the top and in the bottom as well as at the back of the sector had been assumed.

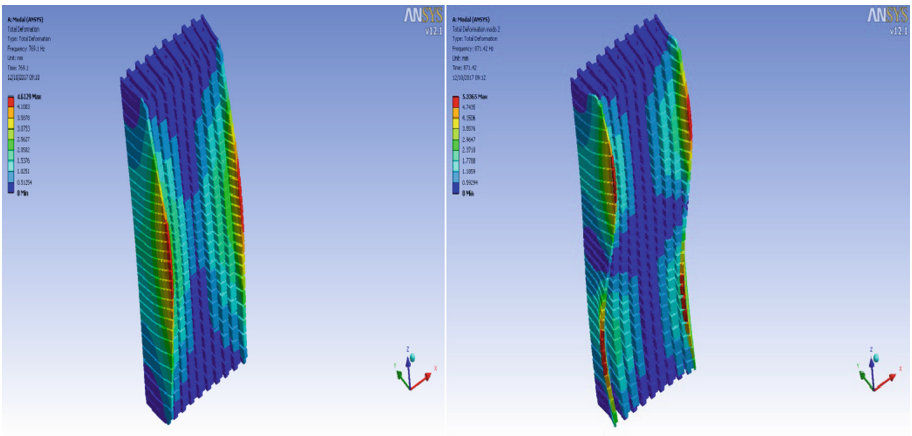

Fig. 13. Vibration modes of one sector of the stator pack: left at 769 Hz right at 871 Hz

Figure 13 shows two mode shapes respectively at 769 Hz and 871 Hz which at least demonstrate that the structure with more realistic boundary conditions could vibrate with similar shapes at a lower frequency, such as the measured frequency of 700 Hz.

Another analysis made by a consultant company (EOMYS Engineering) was focused on the electromagnetic forces acting in the air gap and on the modal analysis of the free standing stator package (without casing). The mode with 0 nodal diameters in axial direction and 22 nodal diameters in circumferential direction resulted at the frequency of 708 Hz (very close to 700 Hz). This mode was strongly coupled with the rotating shaft equipped with 22 pole pairs, that generates a periodical magnetic force distribution over one rotation with 22 maxima and minima, in other words a harmonic component of order 22. The result is a rather strong excitation of the stator in resonance. In this case the consultant company completed the analysis with the evaluation of the stator pack vibrations excited in resonance by the calculated rotating electromagnetic forces, as well as with the evaluation of the emitted noise, getting good agreement with measured data.

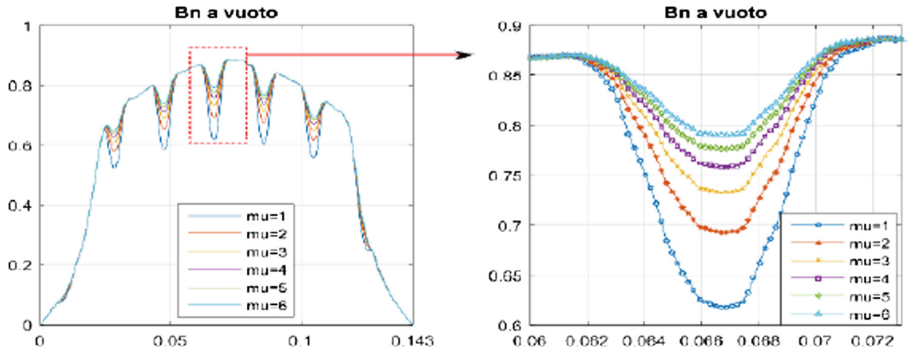

Fig. 14. Magnetic flux versus angular displacement, for different values of slot wedge magnetic permeability mu. Left 1/44 of rotation, right enlargement over one slot.

Since the amplitude of the magnetic force periodical irregularity depends on the magnetic permeability of the wedges in the stator slots, it was proposed to change its material in order to increase its permeability for reducing the irregularity and the strength of excitation. The possibility of changing the frequency of excitation or the natural frequency of the stator pack was discarded, due to obvious reasons.

Figure 14 shows the magnetic flux amplitude as function of the angular position in case of no load, for different values of magnetic permeability. Strong reduction flux amplitude can be obtained with a permeability 6 times higher than its value in air. This corresponds to a still higher reduction of the force acting on the stator, but in case of full load of the generator this reduction tends to vanish due to the interaction with the stator electromagnetic field.

It is not known if this modification has been adopted, or if the noise problem has been solved by passive noise control techniques. The vibration amplitudes of the components at this high frequency are so small (less than 1 μm) that mechanical damage has not been taken into account by the machine manufacturer.

3 Conclusions

Four cases of different malfunctions in different industrial machinery that have been analyzed without diagnostic tools and, at least in three of the cases, without resorting to specific machine and malfunction models, are presented.

In the first three cases the analyses have been possible due to previous experiences in simulations of malfunctioning machines and/or model based identification methods referred also in literature. In the last case the complete diagnostic procedure has been developed including also validation by means of simulation with suitable models.

Although new achievement is not disclosed in this paper, the author believes that experimental results in real industrial machinery are always worthy to be published, when they can be associated to possible, probable or, at the best, identified malfunctions.

References

1. Pennacchi, P., Bachschmid, N., Vania, A.: A model-based identification method of transverse cracks in rotating shafts suitable for industrial machinery. Mech. Syst. Sig. Process. **20**(8), 682–701 (2006)
2. Bachschmid, N., Pennacchi, P., Vania, A.: Identification of multiple faults in rotor systems. J. Sound Vib. **254**(2), 327–366 (2002)
3. Bachschmid, N., Pizzigoni, B., Tanzi, E.: On the 2xrev vibration components in rotating machinery excited by journal ovalization and oil film non-linearity. In: Proceedings of IMechE 7th International Conference on Vibrations in Rotating Machinery, pp. 449–458 (2000)
4. Pennacchi, P., Vania, A.: Analysis of the shaft thermal bow induced by rotor-to-stator rubs. IASME Trans. **1**(1), 193–198 (2004)
5. Walker, J.H., Kerruish, M.A.: Open circuit noise in synchronous machines. Proc. Inst. Electr. Eng. **107**(part A, n° 36), 505–512 (1960)
6. McGuire, M.: Steam turbine vibration characteristics. In: ROVSING Symposium (2004)